



Encapsulation of methotrexate loaded magnetic microcapsules for magnetic drug targeting and controlled drug release



Prabu Chakkarapani^a, Latha Subbiah^{a,*}, Selvamani Palanisamy^a, Arputha Bibiana^a, Fredrik Ahrentorp^b, Christian Jonasson^b, Christer Johansson^b

^a Department of Pharmaceutical Technology & Centre for Excellence in Nanobio Translational Research, Anna University, Bharathidasan Institute of Technology Campus, Tiruchirappalli 620024, Tamil Nadu, India

^b Acreo Swedish ICT AB, Arvid Hedvalls backe 4, SE-411 33 Göteborg, Sweden

ARTICLE INFO

Article history:

Received 30 June 2014

Received in revised form

3 November 2014

Accepted 4 November 2014

Available online 25 November 2014

Keywords:

MMC

Methotrexate

Polyelectrolyte

Layer-by-layer

Rheumatoid arthritis

ABSTRACT

We report on the development and evaluation of methotrexate magnetic microcapsules (MMC) for targeted rheumatoid arthritis therapy. Methotrexate was loaded into CaCO₃-PSS (poly (sodium 4-styrenesulfonate)) doped microparticles that were coated successively with poly (allylamine hydrochloride) and poly (sodium 4-styrenesulfonate) by layer-by-layer technique. Ferrofluid was incorporated between the polyelectrolyte layers. CaCO₃-PSS core was etched by incubation with EDTA yielding spherical MMC. The MMC were evaluated for various physicochemical, pharmaceutical parameters and magnetic properties. Surface morphology, crystallinity, particle size, zeta potential, encapsulation efficiency, loading capacity, drug release pattern, release kinetics and AC susceptibility studies revealed spherical particles of ~3 μm size were obtained with a net zeta potential of +24.5 mV, 56% encapsulation and 18.6% drug loading capacity, 96% of cumulative drug release obeyed Hixson-Crowell model release kinetics. Drug excipient interaction, surface area, thermal and storage stability studies for the prepared MMC was also evaluated. The developed MMC offer a promising mode of targeted and sustained release drug delivery for rheumatoid arthritis therapy.

© 2014 Elsevier B.V. All rights reserved.

1. Introduction

Drug delivery research aims to conveniently administer complex drugs to the target tissue in the biological system in a more stable and reproducible controlled way so that it would achieve higher activity at a minimal dose for prolonged period at the site devoid of side effects. Entrapment of a drug into a polymeric system may protect the drug from inactivation and help to retain its activity for prolonged durations, decrease its toxicity, dosing frequency and offers flexibility in administration. Hollow polymer capsules with definite structures and controlled properties have attracted much attention due to their potential applications in diverse areas, including artificial cells, biotechnology, drug delivery [1]. Several approaches have been established to fabricate capsules made of polymer, such as phase-separation, emulsion polymerization and layer-by-layer (LbL) templating technique [2,3]. The LbL templating technique is a highly versatile approach to prepare micro/nanometer sized capsules with tailored properties. The process involves the step-wise deposition of species onto

a core, which is subsequently removed to generate free-standing capsules [4]. The sequential formation of these capsules is based on the facile selection of sacrificial templates [5–7] and assembly components [7–16]. Various active compounds can be sequestered in to the capsule shell [17,18] and/or interior [19,20] for drug delivery and various other applications. Generally biodegradable and bioabsorbable matrices are preferred so that they would degrade inside the body by hydrolysis or by enzymatic reactions.

Study of the control of microcapsule properties of varying shell composition and physicochemical parameters of the surrounding medium for encapsulation of substances and their controlled release was already published. However, many applications also require remote control over permeability of the microcapsule shell [21]. Introducing magnetic particles makes it possible to remotely control the permeability of their shells and for the shift of microcapsules to the target site [22].

Magnetic drug targeting is the pioneering concept proposed by Freeman et al. in 1960 [23]. This has become a very attractive field of research in which fine iron particles could be transported through the vascular system and concentrated at a particular point in the body with the aid of magnetic fields to achieve prolonged release with high, localized concentrations of drug by retention of the carriers in the region of interest [24].

* Corresponding author. Fax: +91 4312407333.

E-mail address: lathasuba2010@gmail.com (L. Subbiah).

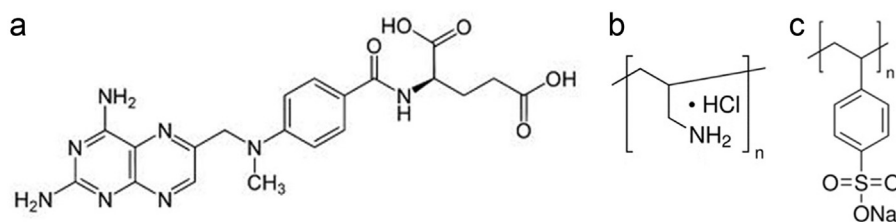


Fig. 1. (a) Structure of methotrexate. (b) Structure of poly (allylamine hydrochloride). (c) Structure of poly (sodium 4-styrenesulfonate).

Methotrexate (Fig. 1a) is a folic acid antagonist, an anti-proliferative and immunosuppressive agent. It is the drug of choice in the treatment of the rheumatoid arthritis, an autoimmune disease. Methotrexate has an extensive toxicity range and adverse reactions that include gastrointestinal, hepatic, renal, pulmonary, and haematological disturbances that may also affect the central nervous system [25]. This lack of efficacy is due to the fact that large amounts of the administered methotrexate are rapidly eliminated by the kidneys, resulting in a short plasma half-life and low drug concentration in the targeted tissue [26].

Recently, CaCO₃-based colloidal templates have been shown to be promising for the synthesis of hollow polyelectrolyte capsules as CaCO₃ is nontoxic and the CaCO₃ core material can be easily removed by complexation with ethylene diamine tetra acetic acid (EDTA). Moreover, CaCO₃ particles are easy to synthesize and are easily filled with macromolecules up to a size of about 40 nm, owing to their high porosity [27].

Hence, to overcome these disadvantages and to improve the pharmacokinetic properties, methotrexate was encapsulated in porous calcium carbonate core which is a biocompatible and decomposable template over coated with biocompatible cationic polyelectrolyte poly (allylamine hydrochloride) (PAH) (Fig. 1b) and anionic polyelectrolyte poly (sodium 4-styrenesulfonate) (PSS) (Fig. 1c) alternatively [28,29]. Ferrofluid was ingrained between the multiple layers of polyelectrolytes. Consequently the calcium carbonate core was etched using EDTA yielded the methotrexate MMC. The physicochemical, pharmaceutical and magnetic properties for the prepared MCs were evaluated and presented. The developed MMC would have a substantially prolonged half-life in the circulation could be magnetically targeted with improved efficacy and reduced adverse effects.

2. Experimental section

2.1. Materials

All chemicals were of analytical reagent grade and were used without any further purification. Methotrexate was a gift received from M/s. Madras Pharmaceuticals Pvt. Ltd, Chennai. Poly (allylamine hydrochloride) (PAH) Mw~58,000 and Poly (sodium 4-styrene sulfonate) (PSS) Mw~70,000 were supplied by Sigma Aldrich. All other chemicals were from Loba Chemie, Mumbai.

2.2. Preparation of methotrexate magnetic microcapsules

2.2.1. Preparation of CaCO₃-PSS microparticles

The CaCO₃-PSS microparticles were prepared by biomimetic mineralization method reported by Zheng Lu et al. [30] with slight modifications. Briefly, by rapidly mixing of (i) 0.2 M Na₂CO₃ in 100 mL water containing 400 mg of PSS with (ii) 0.2 M CaCl₂ in 100 mL water followed by stirring in a stirrer (Remi, 5MLH DX, India) for 30 min. CaCO₃-PSS microparticles were filtered out, repeatedly washed with water finally with acetone and dried in a vacuum oven (Bio Niik Innovation, India) for 1 h at 50 °C.

2.2.2. Drug loading on CaCO₃-PSS microparticles

Methotrexate was loaded to CaCO₃-PSS microparticles using solvent evaporation technique [31]. 200 mg of methotrexate was dissolved in 10 mL of alkali hydroxide solution. Drug solution was added to prepared microparticles of CaCO₃-PSS (400 mg) that was previously dispersed in absolute ethanol and kept under stirring (400 rpm) at room temperature for 12 h. Particles were collected by centrifugation (Eppendorf, 5430 R, India), and dried in a vacuum oven for 1 h at 50 °C.

2.2.3. Preparation of ferrofluid

Stable Fe₃O₄ ferrofluid was synthesized by co-precipitation method using Fe (II) and Fe (III) salts [32]. A solution of FeCl₃·6H₂O and FeCl₂·4H₂O in 2:1 ratio was then quickly charged and mixed together along with an excess amount of 3 M NaOH solution using a mechanical stirrer, under nitrogen atmosphere until the pH value reaches 11 and a black precipitate was obtained. Polyethylene glycol (1 g) was added to this and aged at 80 °C for 60 min and neutralized to pH 7.

2.2.4. Preparation of magnetic microcapsules

MMC were obtained after three steps viz., (i) Deposition of multiple layers of PAH/PSS alternatively onto the surface of drug loaded CaCO₃-PSS microparticles. (ii) Incorporation of ferrofluid between polyelectrolyte layers (iii) Etching of calcium carbonate core. The scheme of preparation was described in (Fig. 2).

The drug loaded CaCO₃-PSS microparticles were coated with cationic and anionic polyelectrolytes by layer-by-layer technique alternatively using PAH and PSS respectively. PAH/PSS polyelectrolyte solution (2 mg/mL) was prepared using 0.5 M NaCl and the pH of the solution was adjusted to 6.5. Each adsorption cycle includes addition of CaCO₃-PSS microparticles (200 mg) to polyelectrolyte solution (5 mL) for 15 min, separation by centrifugation and washing with 0.001 M NaCl solution in sequence. We preferred to have a polycation as the outermost layer as the positive surface charge should enhance the cellular uptake of the capsules, considering that most cell types exhibit a negative surface charge. The multilayer build-up was followed by measuring the zeta potential of the particles after each adsorption step.

Ferrofluid 500 μL (1.2 mg/mL) was added to the coated CaCO₃-PSS microparticles (200 mg) and vortexed (Tarsons, Spinix MC-01, India) for 15 min, separation by centrifugation. The afore-said assembly procedure was continued for more alternate layer of polyelectrolyte was deposited on the above product.

The drug-ferrofluid incorporated CaCO₃-PSS microparticles were incubated together with 0.2 M of EDTA solution maintained at pH 7.0 for 30 min in order to dissolve the CaCO₃-PSS core. Core etched MMC were collected by centrifugation, and dried in a vacuum oven for 1 h at 50 °C and stored for further studies [33].

2.3. Evaluation studies

Evaluation studies were carried out to determine the various physicochemical, pharmaceutical and magnetic properties either for the raw materials, intermediate products or for final products

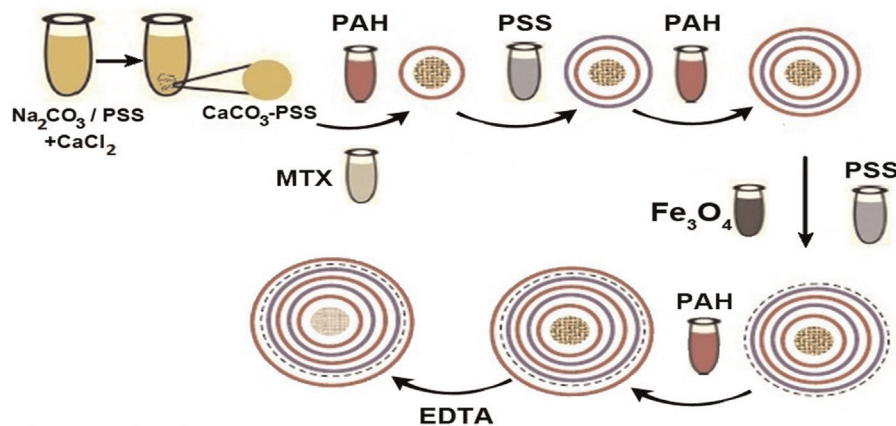


Fig. 2. Scheme for the preparation of methotrexate magnetic microcapsules.

at various stages in confirmation of the experimental protocol and the results were presented appropriately.

2.3.1. Physicochemical characterization

2.3.1.1. Surface morphology. The surface morphology of the $\text{CaCO}_3\text{-PSS}$ microparticle and polyelectrolyte coated methotrexate loaded $\text{CaCO}_3\text{-PSS}$ particles was studied by scanning electron microscopy (JEOL-JSM 6701-F, Japan) upon sputter coating with a thin layer of palladium gold alloy [34]. Few drops of diluted ferrofluid preparation were deposited onto a carbon coated copper grid and the grid was allowed to air dry. TEM (TECHNAI 10-Philips, Netherland) images of ferrofluid were obtained at 60 kv.

2.3.1.2. Surface area. The surface area and pore volume distribution of $\text{CaCO}_3\text{-PSS}$ microparticles and drug loaded microparticles were determined by following the Brunauer-Emmett-Teller (BET) method of nitrogen adsorption, the data being collected with Micromeritics, USA [35]. The nitrogen sorption experiments were performed at 77 K. Prior to the measurement, the samples were outgassed at 120 °C for at least 6 h. The specific surface areas were calculated using adsorption data at a relative pressure range of P/P_0 -0.0000-1.0000.

2.3.1.3. Crystallinity. X-ray diffraction (XRD) patterns for the $\text{CaCO}_3\text{-PSS}$ microparticles were recorded on a Rigaku Ultima III, USA powder diffraction system using $\text{Cu K}\alpha$ radiation of 0.15406 nm wavelength at a scanning rate of 0.02 °/s in the 2θ range of 10–80° [36].

2.3.1.4. Particle size and Zeta potential. The average particle size, polydispersity index and the zeta potential were measured with a Zetasizer Nano ZS, Malvern Instruments, Malvern, UK, Ver. 7.02. Freshly prepared MMC were dispersed in deionized water (5 ml) and placed in a dip cell to eliminate the effect of viscosity caused by the ingredients. The measurement was carried out using a 4 mW He-Ne laser (633 nm) as light source at a fixed angle of 175. The following parameters were used for experiments: medium refractive index 1.300, medium viscosity 0.8872 cP and temperature 25 °C. ζ -Potential was measured with a combination of laser Doppler velocimetry and phase analysis light scattering (PALS). A Smoluchowsky constant F (Ka) of 1.5 was used to calculate potential values from the electrophoretic mobility. Results obtained were the average of three measurements at 25 °C.

2.3.1.5. Drug excipient interaction. The FT-IR spectrum was recorded on Jasco 6300 FT-IR Spectrophotometer, Japan for $\text{CaCO}_3\text{-PSS}$ microparticles, methotrexate, ferrofluid and methotrexate MMC [31]. The samples were prepared by grinding

samples (5 mg) with KBr (100 mg) and then pressing the mixtures into pellets, further placed on to a crystal sample holder and scanned from 4000 to 400 cm^{-1} at a resolution of 2 cm^{-1} .

2.3.2. Pharmaceutical characterization

2.3.2.1. Encapsulation efficiency and Loading capacity. Methotrexate (200 mg) was added to the $\text{CaCO}_3\text{-PSS}$ microparticles (600 mg) in 20 ml of absolute ethanol and was allowed to stand for 24 h for drug loading. The dispersion was centrifuged at 2000 rpm for centrifugal separation and the supernatant was separated. The amount of drug remained in the supernatant was determined by analysis in an UV-Visible spectrophotometer (UV 1800 Shimadzu, Singapore) at 305 nm [38]. The percent encapsulation efficiency was calculated as mentioned below

$$\text{Encapsulation efficiency(\%)} = \left[1 - \frac{\text{Drug in supernatant(mg)}}{\text{Total drug added(mg)}} \right] \times 100$$

MMC (200 mg) were digested in aqueous medium i.e., 20 ml of phosphate buffer pH – 7.5 by mild ultrasonication (Model: 3.5 L 100 H, PCI analytics, Mumbai) and the solution was centrifuged at 2000 rpm for 30 min. The amount of methotrexate in MMC was determined as the difference between the total amount of drug used to prepare the MMC and the amount of drug present in the aqueous medium [38]. The percent drug loading capacity was calculated as mentioned below

$$\text{Drug loading(\%)} = \left[\frac{\text{Methotrexate in Microcapsules(mg)}}{\text{Microcapsules Recovered(mg)}} \right] \times 100$$

2.3.2.2. Drug release pattern and release kinetics. The *in-vitro* drug release studies of methotrexate MMC were performed by the dialysis method in an open end tube sealed dialysis membrane (Himedia Laboratories Pvt. Ltd., Mumbai, India; core diameter-2.4 mm) [39]. The dialysis tube was fitted in an USP dissolution apparatus containing 1000 ml of buffer solution as dissolution medium at pH 7.0, stirred at 60 rpm at 37 °C. MMC (200 mg) were added into the dialysis tube and aliquots of buffer (1 mL) were withdrawn at predetermined time intervals from the external release medium for a period of 36 h and replaced by the same volume of fresh buffer. Absorbance of the withdrawn aliquots was measured using a double beam UV-visible spectrophotometer at 305 nm. The amount of drug present in each aliquot was determined from the standard calibration curve. Data obtained from *in-vitro* release studies were fitted to the various kinetic equations, i.e., zero order, first order, Hixson-Crowell and Higuchi equation. The release mechanism was evaluated with Peppas equation.

2.3.2.3. Thermal stability studies. The thermal stability of CaCO_3 -PSS particles, methotrexate loaded CaCO_3 -PSS particles and polyelectrolyte coated CaCO_3 -PSS particle was examined using thermo gravimetric analyser (TGA) (TA Instruments, Model Q50, USA). The thermograms were obtained in a temperature range from 30 °C to 600 °C at a heating rate of 20 °C/min under nitrogen atmosphere (200 mL/min) [31].

2.3.2.4. Storage stability studies. The formulated MMC were subjected to stability studies in amber and transparent airtight glass containers to assess the stability of the prepared formulation with respect to drug content and drug release characteristics after storing the multiple-units of the formulation in drug stability testing chamber (Model: WIL-195, Wadegati Labequip Pvt. Ltd., India) whilst, stress conditions like temperature was maintained at 25 °C and 65% relative humidity to represent temperate conditions for 60 days [39].

2.3.3. Magnetic characterization

2.3.3.1. Vibrating Sample Magnetometer. Magnetization versus field was measured using VSM analysis with a system from Lakeshore,

USA; Model 7404. VSM measurements were carried out of the dried ferrofluid and of the integrated ferrofluid in the MMC particles (dried sample) at 300 K [40].

2.3.3.2. AC susceptibility. The dynamic magnetic susceptibility measurements (i.e., AC magnetic susceptibility versus frequency) were carried out using the DynoMag system (Acreo Swedish ICT AB, Sweden) in a frequency range of 5–100 kHz. The AC susceptibility is given as the volume susceptibility (SI units) [39].

2.4. Results and discussion

2.4.1. Preparation of methotrexate magnetic microcapsules

MMC were successfully prepared after loading methotrexate and ferrofluid in porous CaCO_3 -PSS microparticles, that were overcoated with alternate layers of using PAH and PSS by layer-by-layer technique. The number of layers coated was chosen arbitrarily. Finally the CaCO_3 -PSS core was removed by etching with EDTA. Porous CaCO_3 -PSS microparticles were prepared by biomimetalisation method. PSS, a strong polyanion, tightly binds Ca^{2+}

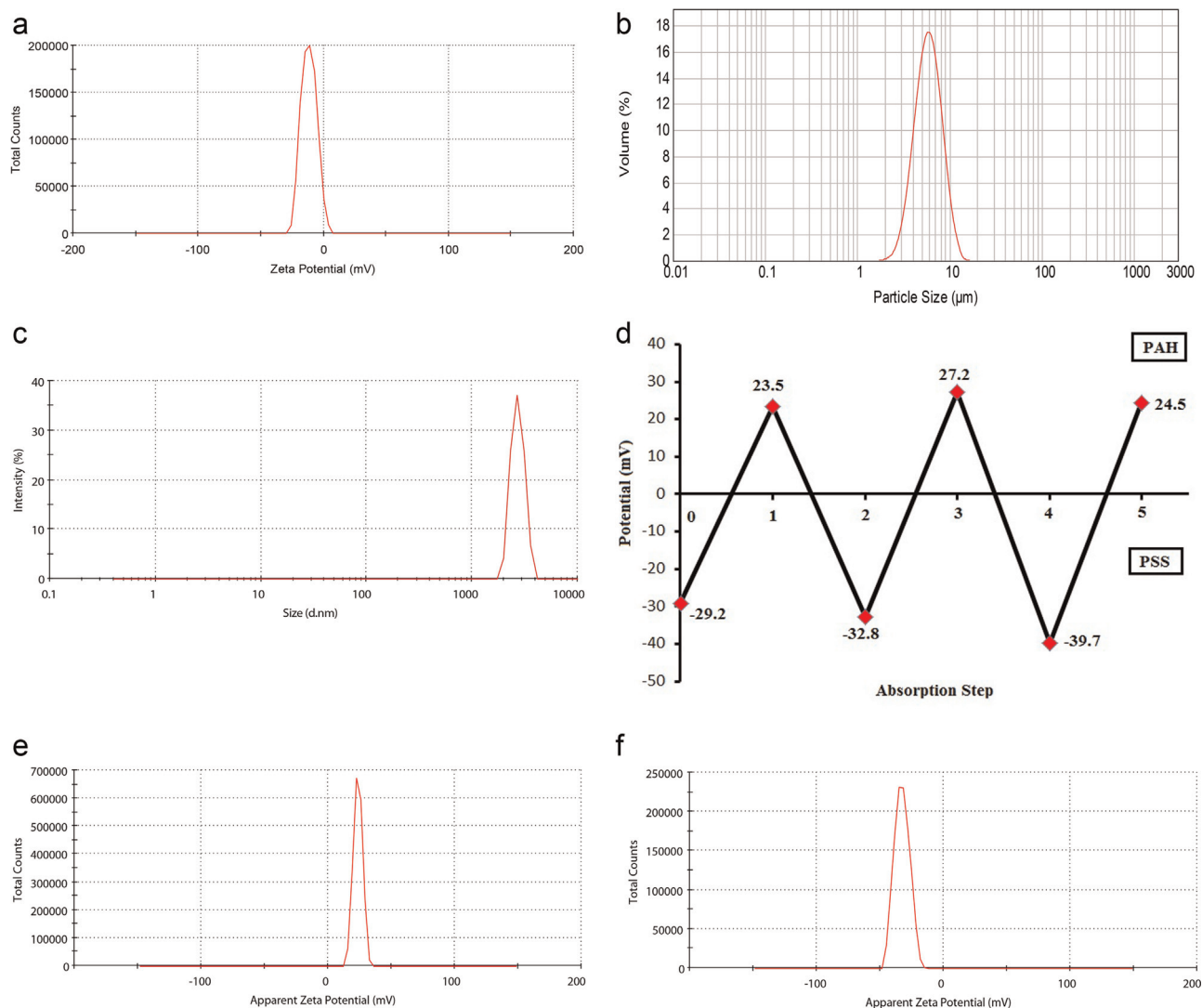


Fig. 3. (a) Zeta potential of CaCO_3 - PSS microparticles. (b) Particle size distribution of CaCO_3 - PSS microparticles. (c) Size distribution of methotrexate magnetic microcapsules. (d) Variation of zeta potential after addition of alternative polyelectrolyte over CaCO_3 - PSS microparticles. (e) Variation of zeta potential after addition of PAH polyelectrolyte over CaCO_3 - PSS microparticles (Layer - 1). (f) Variation of zeta potential after addition of PSS polyelectrolyte over CaCO_3 - PSS microparticles (Layer - 2). (g) Variation of zeta potential after addition of PAH polyelectrolyte over CaCO_3 - PSS microparticles (Layer - 3). (h) Variation of zeta potential after addition of PSS polyelectrolyte and ferrofluid over CaCO_3 - PSS microparticles (Layer - 4). (i) Apparent zeta potential of ferrofluid. (j) Variation of zeta potential after addition of PAH polyelectrolyte over CaCO_3 - PSS microparticles (Layer - 5).

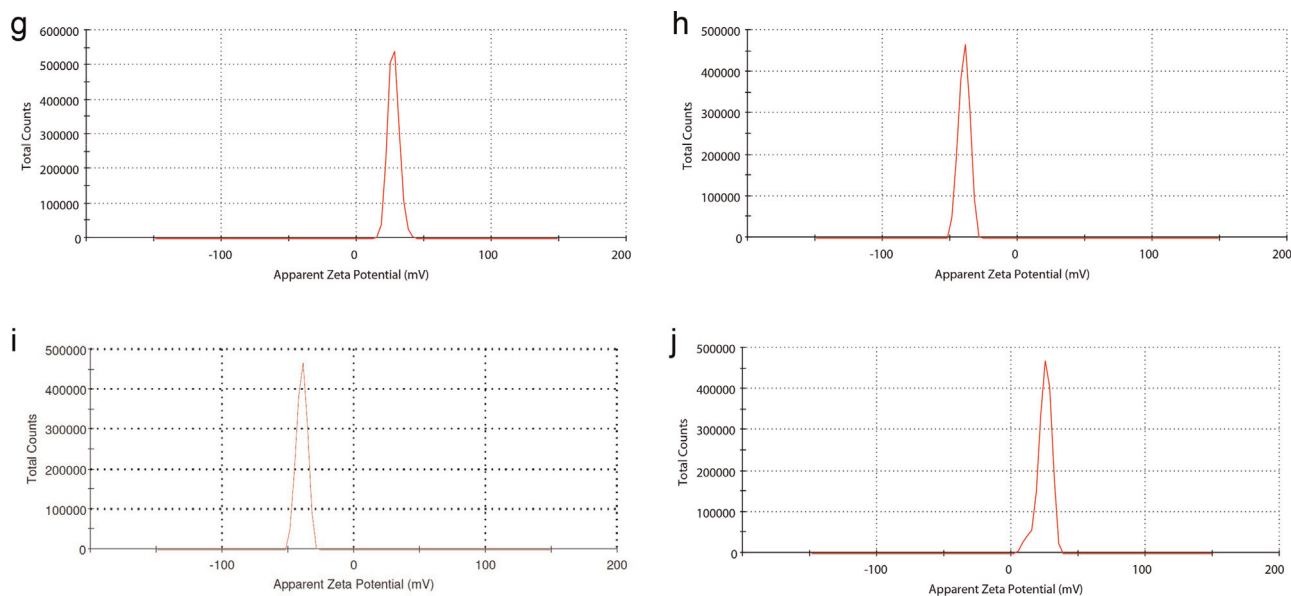


Fig. 3. (continued)

ions, and thereby decreases free Ca^{2+} ion concentration and slows down growth rate of CaCO_3 particles. PSS precipitates along with the Ca ions and the repulsive electrostatic forces exist between CaCO_3^{2-} and PSS ions result in the formation of pores throughout the CaCO_3 -PSS microparticles. PSS at high concentration is a strong nucleation inhibitor for calcium carbonate. This means that the crystallization of calcite and vaterite from many precursors is slowed down. Nevertheless, the CO_3^{2-} has a stronger binding

strength to Ca^{2+} . Thermodynamically, they are favourable to combine with the Ca^{2+} ions, which are highly localized and enriched near the PSS backbone. Due to the interference of sulfonate group and the polymer backbone, microparticles were easily formed and stabilized in situ by PSS. It was further demonstrated that the microparticles thus obtained were stable vaterite crystal structure [41,42] and exhibited a zeta potential of -11 mV (Fig. 3a). The prepared CaCO_3 – PSS particles were found to be

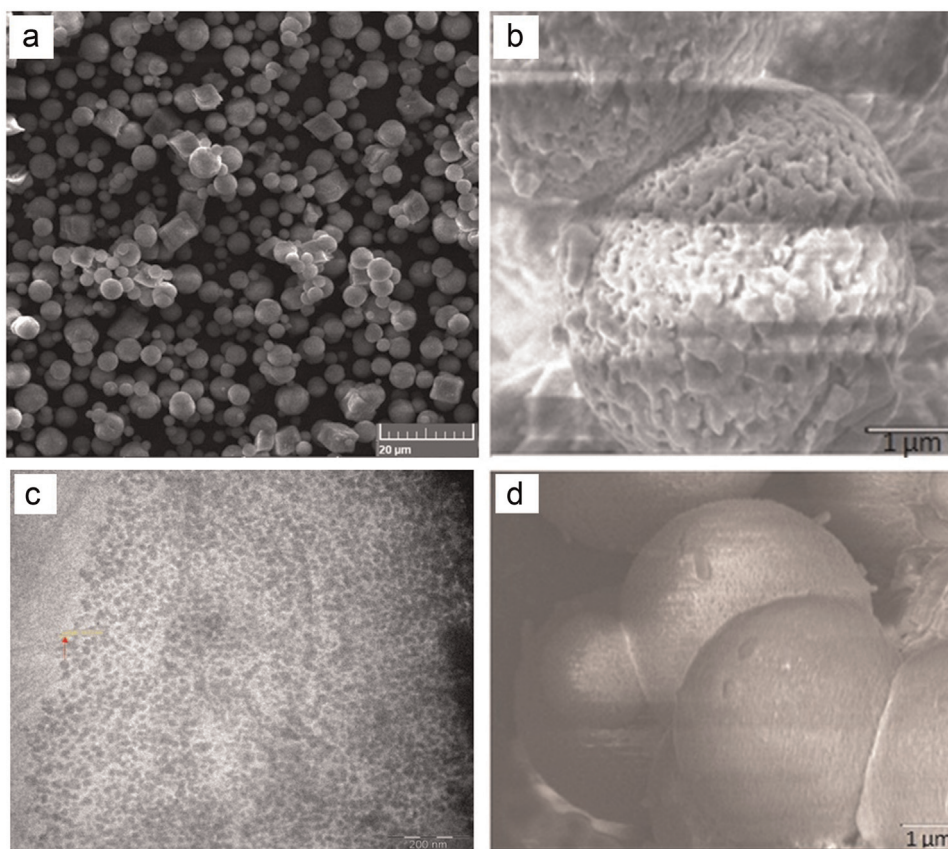


Fig. 4. (a) SEM micrograph of CaCO_3 – PSS microparticles. (b) SEM micrograph of CaCO_3 – PSS microparticle having porous surface. (c) TEM image of magnetite nanocrystals in the ferrofluid. (d) SEM micrograph of methotrexate magnetic microparticles having smooth surface.

~5 μm (Fig. 3b) and exhibited spherical and porous morphology as evidenced from the SEM micrographs (Fig. 4a & b). The magnetite particles in the ferrofluid exhibited ~40 nm as evidenced from the TEM analysis (Fig. 4c).

2.5. Evaluation studies

2.5.1. Physicochemical characterization

2.5.1.1. Surface morphology. The prepared MMC exhibited a spherical and smooth surface morphology evidenced through SEM analysis (Fig. 4d). Coating with multiple layers of the polyelectrolytes over the porous CaCO_3 -PSS microparticles turns the porous surface to a smoother surface. This is due to slight conglutination occurring among them that owes to bridging of oppositely charged polyelectrolytes adsorbed over each other. The surface looks quite rigid perhaps due to the incorporation of magnetite between the polyelectrolyte layers [31].

2.5.1.2. Surface area. The method of multipoint Brunauer-Emmett-Teller (BET) is used to determine the total surface area and the isotherms for CaCO_3 -PSS and methotrexate loaded CaCO_3 -PSS microparticles. The BET isotherms of CaCO_3 -PSS and methotrexate loaded CaCO_3 -PSS microparticles were shown in (Fig. 5). The multipoint BET data from the above isotherms revealed that the volume of adsorption of CaCO_3 -PSS microparticles before drug loading is 0.38, 0.49, 0.54, 0.85, 1.13 and the volume of adsorption has been reduced as 12.68, 14.07, 15.24, 16.23, 17.24 upon analysis after drug loading. The surface area has been reduced from $6.16\text{E}+00 \text{ m}^2/\text{g}$ to $5.36\text{E}+01 \text{ m}^2/\text{g}$ hints that the pores were occupied by methotrexate. The above data is in accordance with the results of percentage encapsulation efficiency, percentage drug loading and drug assay that proves the drug molecules could penetrate into the pores of CaCO_3 -PSS microparticles. The obtained results are in agreement with other similar studies [35].

2.5.1.3. Crystallinity. X-ray diffraction pattern (Fig. 6) of calcium carbonate was similar with the report of crystal lattice calcium carbonate shown by Raz et al. [43]. As a primary characterization tool X-ray diffraction patterns have been widely used in nanoparticle research for obtaining critical features such as crystal structure, crystallite size, and strain. The randomly oriented crystals in nano crystalline materials cause broadening of diffraction peaks. This has been attributed to the absence of total constructive and destructive interferences of X-rays in a finite sized lattice.

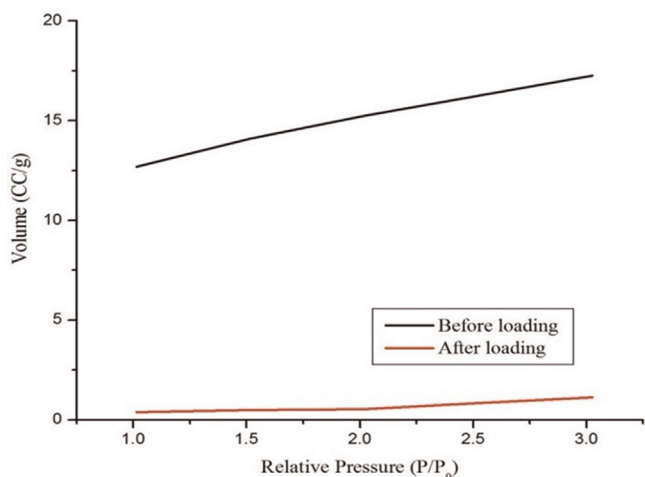


Fig. 5. BET isotherm of CaCO_3 -PSS microparticles & BET isotherm of methotrexate loaded CaCO_3 -PSS microparticles.

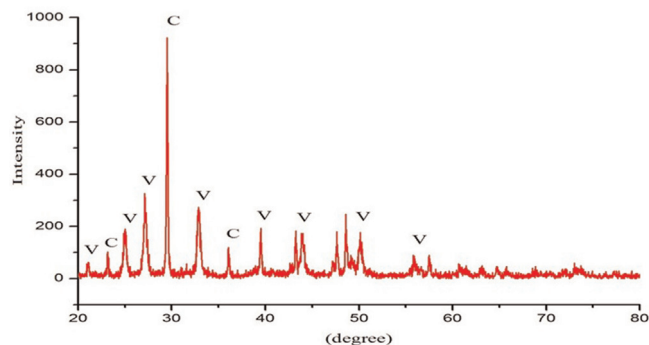


Fig. 6. XRD pattern of CaCO_3 -PSS microparticles.

Moreover, inhomogeneous lattice strain and structural faults lead to broadening of peaks in the diffraction patterns [44]. The diffractogram shows that the CaCO_3 -PSS microparticles had a dominant phase of vaterite and trace amount of calcite. The broadening diffraction peaks suggests that the produced vaterite microspheres were composed of numerous tiny particles and found to be in amorphous state [36,37].

2.5.1.4. Particle size and zeta potential. The mean particle size of the prepared MMC was found to be in the range of 3.53 μm with a polydispersity index of 0.121 (Fig. 3c). The variation in the size of MMC exists due to the hydrolyzation of the PSS present in CaCO_3 [32]. Further, shrinkage in size from ~5 μm to ~3 μm may occur due to the void space formed after dissolution of the CaCO_3 core by EDTA.

Polarity reversal of zeta potential analysed after every layer of polyelectrolyte coating confirms existence of polyelectrolyte layers (Fig. 3d). The variations in zeta potential after addition of alternative polyelectrolyte over CaCO_3 -PSS microparticles are depicted below (Fig. 3e-j). The zeta potential observed for the MMC was found to be +24.5 mV (Fig. 3j). The observed polydispersity index is a good indicator of long-term colloidal stability of the encapsulated MMC.

2.5.1.5. Drug excipient interaction. Drug excipient interaction studies verified through FT-IR spectroscopy revealed that no chemical interaction exists between the methotrexate and used excipients. Further, the spectral group of frequencies confirms the incorporation of methotrexate, ferrofluid and polyelectrolyte in the prepared MMC as their functional groups were intact.

FT-IR spectrum of CaCO_3 -PSS (Fig. 7a) features calcium carbonate phases due to the differences occurring in their carbonate ions (CO_3^{2-}). Carbonate ions and similar molecules have four normal modes of vibration peaks: ν_1 , symmetric stretching; ν_2 , out of plane bending; ν_3 , doubly degenerate planar asymmetric stretching; and ν_4 , doubly degenerate planar bending [45]. The spectral data obtained for the sample reveals a broad absorption peak at 1357 cm^{-1} , 1009 cm^{-1} , 876 cm^{-1} , and 745 cm^{-1} , which have been reported to be the common characteristic features of the carbonate ions in calcium carbonate and are the fundamental modes of vibration for this molecule.

The characteristic peaks of FT-IR spectrum of PAH (Fig. 7b) was observed at 3440 cm^{-1} (Aliphatic amine NH stretch), 1517 cm^{-1} (Aliphatic amine NH bending) and 3031 cm^{-1} (CH_2 stretching). The symmetric and asymmetric bands were observed at 1605 cm^{-1} and 1391 cm^{-1} respectively.

FT-IR spectra of PSS (Fig. 7c) showed peaks at 1184 cm^{-1} , 1130 cm^{-1} and 1040 cm^{-1} ; where peaks at 1184 cm^{-1} , 1040 cm^{-1} could be assigned to the SO_3 group (antisymmetric and symmetric vibrational absorption) and 1130 cm^{-1} to the inplane skeleton vibration of the benzene ring respectively [46].

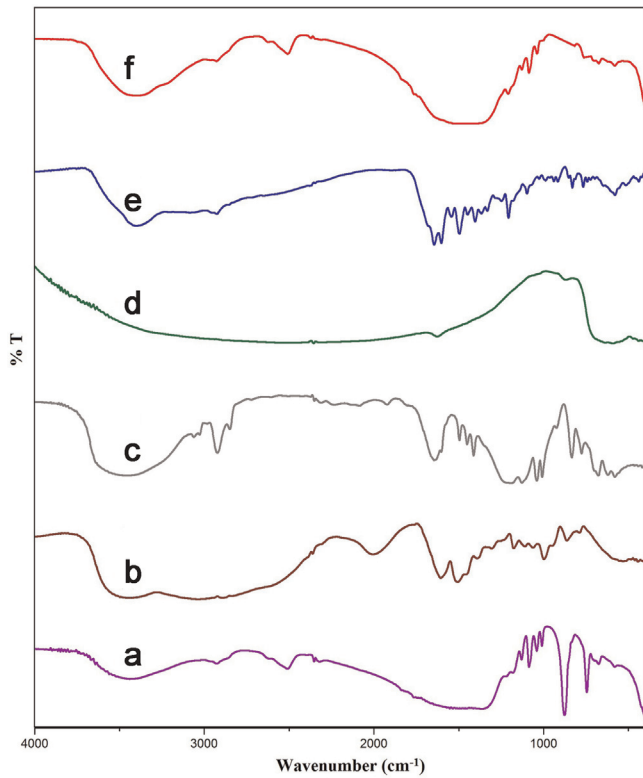


Fig. 7. FT-IR spectrums of (a) CaCO_3 - PSS microparticles. (b) PAH. (c) PSS. (d) Ferrofluid. (e) Methotrexate. (f) Methotrexate magnetic microcapsules.

An infrared spectrum of the ferrofluid (Fig. 7d) was characterized with the bands at 587 cm^{-1} , due to the Fe-O bond in tetrahedral and octahedral positions [47].

FT-IR spectral analysis of methotrexate (Fig. 7e) showed the principal peaks at 1693 cm^{-1} ($-\text{COOH}$), 1643 cm^{-1} ($-\text{CO-NH}$), 1543 cm^{-1} and 1500 cm^{-1} (aryl system) and 830 cm^{-1} (aromatic ring system) confirming the purity of the drug as per established standards [48].

The spectral group frequencies of MMC (Fig. 7f) was characterized at 3396 cm^{-1} (NH stretching), 2928 cm^{-1} , 2507 cm^{-1} , 1501 cm^{-1} (aryl system), 1209 cm^{-1} , 875 cm^{-1} (aromatic ring system) and 744 cm^{-1} , 673 cm^{-1} , 580 cm^{-1} . Peaks associated with the CaCO_3 -PSS core material, showed essentially 100% transmittance after core removal, indicating that the core is completely removed. Furthermore the spectrum does not feature any additional ghost peak that indicates the absence of chemical interaction in the drug loaded MMC.

2.5.2. Pharmaceutical characterization

2.5.2.1. Encapsulation efficiency and loading capacity. The encapsulation efficiency and loading capacity was found to be 56% and 18.6% respectively.

2.5.2.2. Drug release pattern and release kinetics. The drug release study for the MMC has been carried out in dialysis bag with 200 mg of the microcapsules shows the extended release of methotrexate up to 96% over a period of 36 h. In order to determine the release kinetics which best describes the pattern of drug release, the *in-vitro* release data were substituted in equations of zero order, first order, Higuchi and Hixson-Crowell models (Fig. 8a–d). The correlation coefficient values for zero order, first order, Higuchi and Hixson-Crowell models were found to be 0.95, 0.74, 0.98 & 0.99 respectively. Both Hixson-Crowell model and Higuchi model showed best fit to the drug release kinetics based upon the correlation coefficient. The linearity was observed in the square root of time vs cumulative percentage of drug released (Fig. 8c) indicates that the drug release might be occurred from

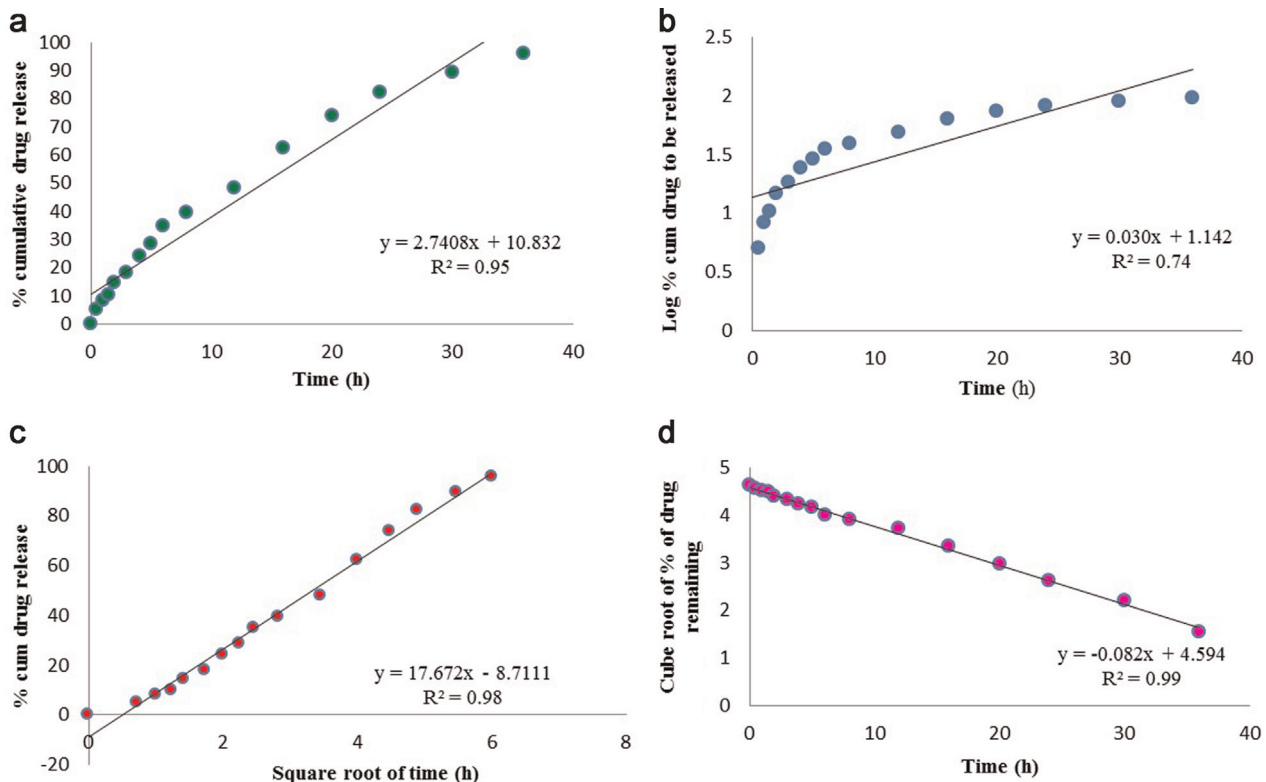


Fig. 8. Cumulative released amount of MMC in different models (a) Zero order model. (b) First order model. (c) Higuchi model. (d) Hixson-Crowell plot.

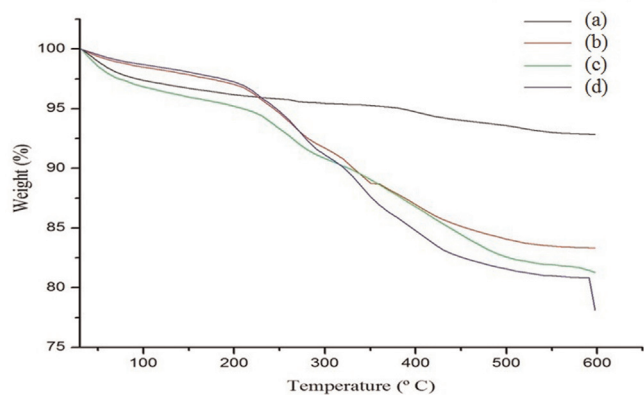


Fig. 9. Thermograms of (a) CaCO_3 - PSS microparticles. (b) Methotrexate loaded CaCO_3 - PSS microparticles. (c) PAH coated methotrexate microparticles. (d) PSS coated methotrexate microparticles.

inner core of the microcapsules through diffusion. On the other hand, the graphical representation of the cube root of the amount remaining versus time will be linear if the equilibrium conditions are not reached and if the geometrical shape of the dosage form diminishes proportionally overtime (Fig. 8d) [49]. For systems in which the surface area and diameter of the drug matrix change with time, the Hixson-Crowell model can be used [50]. Hence, to infer upon the drug release rate from the microcapsules is not only limited by the drug particles dissolution rate but also by the diffusion.

2.5.2.3. Thermal stability studies. Incorporation of drug into microparticles and the thermal stability through TGA thermograms. The TGA thermograms of CaCO_3 -PSS, CaCO_3 -PSS loaded with methotrexate and CaCO_3 -PSS-methotrexate further coated with polyelectrolytes (cationic and anionic) were compared (Fig. 9a – d). The thermal decomposition and related phase transition occurs at 33 °C and at 600 °C showed a weight loss upto 8% in CaCO_3 -PSS microparticles whereas in Methotrexate loaded CaCO_3 - PSS microparticles, the transition occurs at 600 °C and showed 20% weight loss probably due to the decomposition of the drug. The weight loss could be marginally minimised as the number of adsorption cycles of polyelectrolytes was increased [31].

2.5.2.4. Storage stability studies. The results of storage stability studies on various physicochemical and pharmaceutical parameters determined for the MMC performed for 60 days maintained at 25 °C and 65% relative humidity was provided in (Table. 1). No significant changes were observed during the duration of studies.

2.5.3. Magnetic Characterization

2.5.3.1. Vibrating Sample Magnetometer analysis. DC magnetization analysis was carried out using the vibrating sample magnetometer (VSM) technique in order to study the static magnetic properties of the magnetic particles (both the ferrofluid and the MMC particles with integrated ferrofluid) at room temperature. From the

Table 1
Storage stability studies of methotrexate magnetic microcapsules.

S. No	Time (Days)	Size (μm)	Drug Content (%)	Cumulative Drug Release
1	0	3.53	95.33	95.62%
2	15	3.26	95.18	95.40%
3	30	3.19	94.86	95.16%
4	45	2.96	94.39	94.88%
5	60	2.84	93.16	94.23%

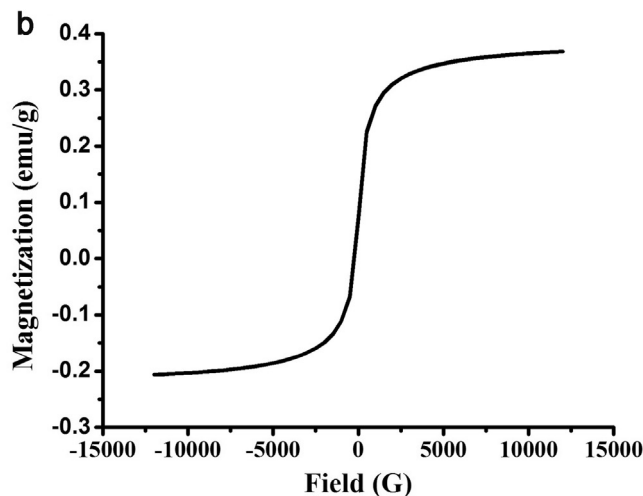
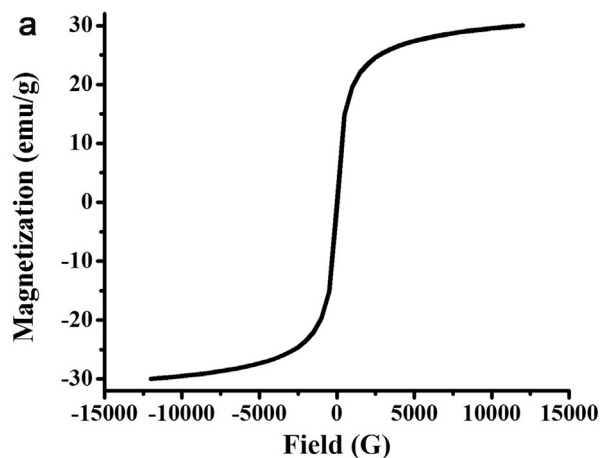


Fig. 10. (a) Magnetization (in emu/g) as a function of magnetic field (in Gauss) of dried ferrofluid. (b) Dried MMC particles at room temperature.

magnetization curve you can determine saturation magnetization of samples and if there is coercivity or remanence in the particle system. (Figs. 10a & b) shows hysteresis curves of the dried ferrofluid (Fig. 10a) and dried MMC particles (Fig. 10b). Taking into account the measured saturation magnetization of the ferrofluid to be 30 emu/g (see Fig. 10a), the magnetic ferrofluid solid content after integration in the MMC particles is about 1% by mass since the saturation magnetization of the MMC particles is about 0.3 emu/g, see Fig. 10b. Magnetization curve confirms an almost superparamagnetic behaviour of MMC, showing a small coercivity of 4 Oe and a low relative remanence of 0.06. This superparamagnetic behaviour in combination with a magnetic ferrofluid solid concentration of about 1% (by mass), makes the magnetic MMC particle system suitable for the proposed applications [51,52] and allows also imaging of the MMC, by means of e.g. magnetic resonance imaging (MRI) or magnetic particle imaging (MPI).

2.5.3.2. AC susceptibility. AC susceptibility (ACS) measurements are an important tool in the characterisation of the magnetic dynamics in magnetic nanoparticle systems. With ACS analysis you can determine which types of magnetic relaxations, Néel or Brownian relaxation, you have in a particle system. The dynamic magnetic response of the MMC particle system in an applied AC magnetic field was measured through the complex susceptibilities the real part χ' and the imaginary part χ'' . The result can be seen in (Fig. 11a). The real component χ' represents the component of the susceptibility that is in phase with the applied AC field, while χ''

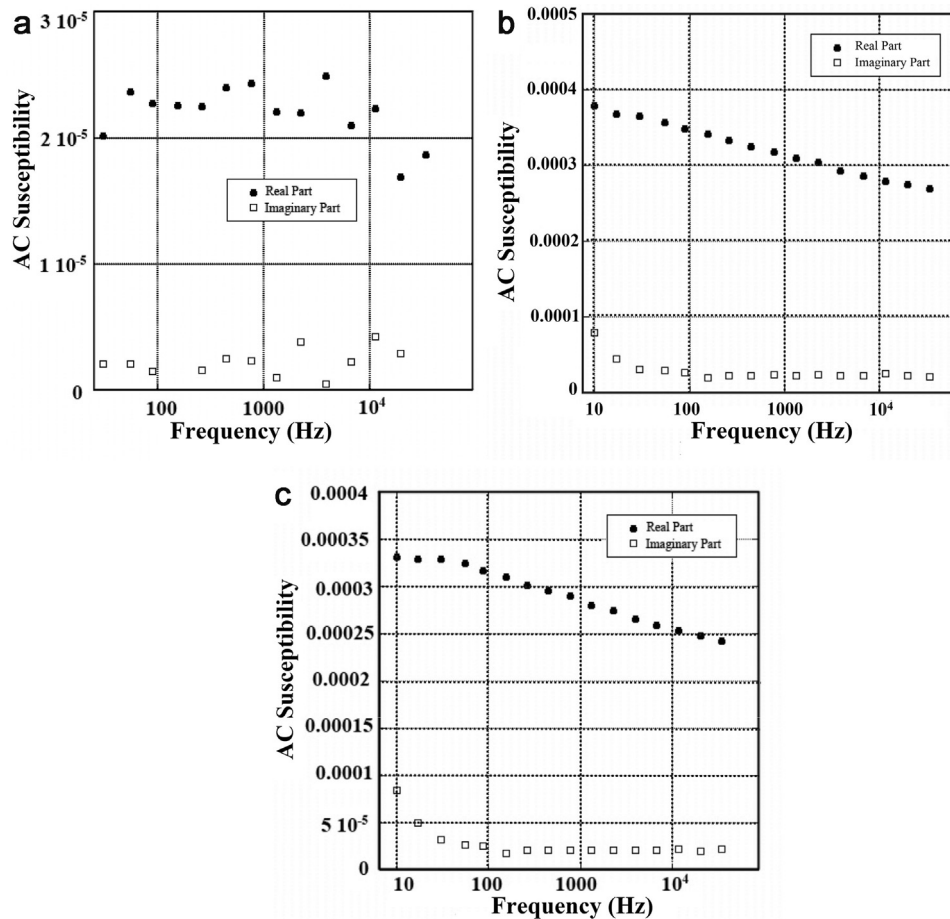


Fig. 11. AC susceptibility versus frequency of three different prepared samples of methotrexate magnetic microcapsules (MMC) (a-c). Measurements were carried out at room temperature and with the MMC particles in carrier liquid (water).

represents the component that is out of phase (the loss part). The very low and constant value of the real part of the AC susceptibility of about $2.25 \cdot 10^{-5}$ between 10–20 kHz is evidence of low concentration of magnetic material in the sample. Furthermore, the χ'' values are close to zero and the absence of a magnetic relaxation peak in the frequency range measured, indicates on that no Brownian relaxation is present above 10 Hz and that the nanocrystals in the MMC particle system relax via the Néel relaxation. There can be a Brownian relaxation frequency peak at low frequencies due to that some of the magnetite nanocrystals have sizes large enough to give a thermally blocked behavior. From the TEM image in (Fig. 4c) we can see that some of the nanocrystals are in the size range of 30 nm–40 nm, which has Néel relaxation times much larger than the Brownian relaxation of the 3 μm MMC particles. The 3 μm MMC particles would give a Brownian relaxation frequency around 16 mHz which is outside the frequency window of the DynoMag system.

The result in (Fig. 11a) shows then that some of the nanocrystals in this MMC particle system exhibit fast Néel relaxation. AC susceptibility measurements of two other MMC particle system samples (Figs. 11b & c) shows that the real part is decreasing in the shown frequency range and that the imaginary part is constant above about 20 Hz and then increasing below 20 Hz. This indicates that the nanocrystals in these MMC particle systems also undergo Néel relaxation but in this case that the nanocrystal relaxation is effected by the changing AC excitation frequency (i.e. that the excitation frequency is close to the Néel relaxation frequency of the nanocrystals) and that this implies that the nanocrystal sizes are larger in these MMC particle system samples than the other

analyzed sample. The increase of the imaginary part below 20 Hz might indicate a low Brownian relaxation frequency due to the stochastic particle rotation of the 3 μm MMC particles (Brownian relaxation frequency of about 16 mHz).

3. Conclusion

In the present work an approach to the successful encapsulation of methotrexate and magnetite by utilizing the ability of adsorption of CaCO_3 -PSS microparticles and further development into multi-layered polyelectrolyte microcapsules has been described. Moreover, the multilayer coating could prolong the release of the loaded methotrexate within the same incubation time. Thus, this system has great application potential for the application of *in-vivo* drug delivery for possible use and application in rheumatoid arthritis magnetic targeted therapy.

Acknowledgements

The work was supported by the research grants sanctioned to Dr.S.Latha and Dr.P.Selvamani from the Defence Research and Development Organization, New Delhi (No. ERIP/ER/0903779/M/01/1249), Government of India. The authors are indebted to Prof. Silvio Dutz, Technische Universität Ilmenau, Germany for critical reading of the manuscript and valuable discussions in interpretation of results. This work utilized facilities supported in part by the Department of Science and Technology, New Delhi Sponsored

National Facility for Drug Development for Academia, Pharmaceutical and Allied Industries, Anna University, BIT Campus, Tiruchirappalli for the particle size cum zeta potential measurements. The authors acknowledge the use of the Central Instrumentation Facility at the Pondicherry University for performing VSM measurements; SASTRA University, Tanjore for SEM and Tamil Nadu Veterinary and Animal Sciences University, Chennai for TEM measurements. The authors acknowledge the honorary support extended by Mr.M.Balasubramanian, U & I media, Tiruchirappalli for preparing quality images for the manuscript.

References

- [1] W. Meier, Polymer nanocapsules, *Chem. Soc. Rev.* 29 (2000) 295–303.
- [2] C.S. Peyratout, L. Dahne, Tailor-made polyelectrolyte microcapsules: from multi-layers to smart containers, *Angew. Chem. Int. Ed.* 43 (2004) 3762–3783.
- [3] Y. Wang, A.S. Angelatos, F. Caruso, Template synthesis of nanostructured materials via layer-by-layer assembly, *Chem. Mater.* 20 (2008) 848–858.
- [4] E. Donath, G.B. Sukhorukov, F. Caruso, S.A. Davis, H. Mohwald, Novel hollow polymer shells by colloid-templated assembly of polyelectrolytes, *Angew. Chem. Int. Ed.* 37 (1998) 2202–2205.
- [5] A.I. Petrov, D.V. Volodkin, G.B. Sukhorukov, Protein-calcium carbonate co-precipitation: a tool for protein encapsulation, *Biotechnol. Prog.* 21 (2005) 918–925.
- [6] F. Wang, J. Feng, W. Tong, C.Y. Gao, A facile pathway to fabricate microcapsules by in situ polyelectrolyte coacervation on poly(styrene sulfonate)-doped CaCO₃ particles, *J. Mater. Chem.* 17 (2007) 670–676.
- [7] T. Borodina, E. Markvicheva, S. Kunizhev, H. Moehwald, G.B. Sukhorukov, O. Kreft, Controlled release of DNA from self-degrading microcapsules, *Macromol. Rapid Commun.* 28 (2007) 1894–1899.
- [8] G. Ibarz, L. Dahne, E. Donath, H. Mohwald, Smart micro- and nanocontainers for storage, transport, and release, *Adv. Mater.* 13 (2001) 1324–1327.
- [9] K.W. Wang, Q. He, X.H. Yan, Y. Cui, W. Qi, L. Duan, J.B. Li, Encapsulated photosensitive drugs by biodegradable microcapsules to incapacitate cancer cells, *J. Mater. Chem.* 17 (2007) 4018–4021.
- [10] A.G. Skirtach, A.M. Javier, O. Kreft, K. Kohler, A.P. Alberola, H. Mohwald, W.J. Parak, G.B. Sukhorukov, Laser-induced release of encapsulated materials inside living cells, *Angew. Chem. Int. Ed.* 45 (2006) 4612–4617.
- [11] B. Zebli, A.S. Susha, G.B. Sukhorukov, A.L. Rogach, W.J. Parak, Magnetic targeting and cellular uptake of polymer microcapsules simultaneously functionalized with magnetic and luminescent nano crystals, *Langmuir* 21 (2005) 4262–4265.
- [12] S. Moya, E. Donath, G.B. Sukhorukov, M. Auch, H. Baumler, H. Lichtenfeld, H. Mohwald, Lipid coating on polyelectrolyte surface modified colloidal particles and polyelectrolyte capsules, *Macromolecules* 33 (2000) 4538–4544.
- [13] Z.H. An, H. Mohwald, J.B. Li, pH controlled permeability of lipid/protein biomimetic microcapsules, *Biomacromolecules* 7 (2006) 580–585.
- [14] L. Duan, Q. He, X.H. Yan, Y. Cui, K.W. Wang, J.B. Li, Hemoglobin protein hollow shells fabricated through covalent layer-by-layer technique, *Biochem. Biophys. Res. Commun.* 354 (2007) 357–362.
- [15] C. Schuler, F. Caruso, Decomposable hollow biopolymer-based capsules, *Biomacromolecules* 2 (2001) 921–926.
- [16] D.G. Shchukin, A.A. Patel, G.B. Sukhorukov, Y.M. Lvov, Nanoassembly of biodegradable microcapsules for DNA encasing, *J. Am. Chem. Soc.* 126 (2004) 3374–3375.
- [17] Z.J. Wang, L. Qian, X.L. Wang, F. Yang, X.R. Yang, Construction of hollow DNA/PLL microcapsule as a dual carrier for controlled delivery of DNA and drug, *Colloid Surf. A* 326 (2008) 29–36.
- [18] Z.J. Wang, L. Qian, X.L. Wang, H. Zhu, F. Yang, X.R. Yang, Hollow DNA/PLL microcapsules with tunable degradation property as efficient dual drug delivery vehicles by-chymotrypsin degradation, *Colloid Surf. A* 332 (2009) 164–171.
- [19] C. Dejugnat, D. Halozan, G.B. Sukhorukov, Defined picogram dose inclusion and release of macromolecules using polyelectrolyte microcapsules, *Macromol. Rapid Commun.* 26 (2005) 961–967.
- [20] G.B. Sukhorukov, H. Mohwald, Multifunctional cargo systems for biotechnology, *Trends Biotechnol.* 25 (2007) 93–98.
- [21] D.A. Gorin, S.A. Portnov, O.A. Inozemtseva, Z. Luklinska, A.M. Yashchenok, A. M. Pavlov, A.G. Skirtach, H.M. hwaldb, G.B. Sukhorukov, Magnetic/gold nanoparticle functionalized biocompatible microcapsules with sensitivity to laser irradiation, *Phys. Chem. Chem. Phys.* 10 (2008) 6899–6905.
- [22] M. Yashchenok, O.A. Inozemtseva, A. Gorin, Nanocomposite microcapsules containing nanoparticles of colloidal gold and magnetite: their preparation and characterization, *Nanotechnol. Russ.* 5–6 (2009) 349–353.
- [23] M.W. Freeman, A. Arrott, J.H.L. Watson, Magnetism in medicine, *J. Appl. Phys.* 31 (1960) S404.
- [24] S.C. Goodwin, C.A. Bittner, C.L. Peterson, G. Wong, Single-dose toxicity study of hepatic intra-arterial infusion of doxorubicin coupled to a novel magnetically targeted drug carrier, *Toxicol. Sci.* 60 (2001) 177–183.
- [25] N. Varatharajan, I.G. Lim, A.A. Coomarasamy, Methotrexate: long-term safety and efficacy in an Australian consultant rheumatology practice, *Intern. Med. J.* 39 (4) (2009) 228–236.
- [26] C. Fiehn, E. Neumann, A. Wunder, S. Krienke, S. GaY, U. Müller-Ladner, Methotrexate (MTX) and albumin coupled with MTX (MTX-HSA) suppress synovial fibroblast invasion and cartilage degradation in-vivo, *Ann. Rheum. Dis.* 63 (2004) 884–886.
- [27] B.G.D. Geest, R.E. Vandenbroucke, A.M. Guenther, G.B. Sukhorukov, W.E. Hennink, N. N. Sanders, J. Demeester, S.C.D. Smedt, Intracellularly degradable polyelectrolyte microcapsules, *Adv. Mater.* 18 (2006) 1005–1009.
- [28] D.B. Shenoy, A. Antipov, G.B. Sukhorukov, H. Mohwald, Layer-by-layer engineering of biocompatible, decomposable core-shell structures, *Biomacromolecules* 4 (2003) 265–272.
- [29] H. Sami, A.K. Maparu, A. Kumar, S. Sivakumar, Generic delivery of payload of nanoparticles intracellularly via hybrid polymer capsules for bioimaging applications, *PLoS One* 7 (5) (2012) e36195.
- [30] Z. Lu, J. Zhang, Y. Ma, S. Song, W. Gu, Biomimetic mineralization of calcium carbonate/carboxy methylcellulose microspheres for lysozyme immobilization, *Mater. Sci. Eng. C* 32 (2012) 1982–1987.
- [31] C. Wang, C. He, Z. Tong, X. Liu, B. Ren, F. Zeng, Combination of adsorption by porous CaCO₃ microparticles and encapsulation by polyelectrolyte multilayer films for sustained drug delivery, *Int. J. Pharm.* 308 (2006) 160–167.
- [32] S. Ghassabian, T. Ehtezazi, S.M. Forutan, S.A. Mortazavi, Dexmethasone loaded magnetic albumin microspheres preparation and in-vitro release, *Int. J. Pharm.* 130 (1996) 49–66.
- [33] S.H. Hu, C.H. Tsai, C.F. Liao, D.M. Liu, S.Y. Chen, Controlled rupture of magnetic polyelectrolyte microcapsules for drug delivery, *Langmuir* 24 (2008) 1181–11818.
- [34] Y. Jin, W. Liu, J. Wang, J. Fang, H. Gao, (Protamine/dextran sulfate)₅ microcapsules templated on biocompatible calcium carbonate microspheres, *Colloid Surf. A* 342 (2009) 40–45.
- [35] C. Peng, Q. Zhao, C. Gao, Sustained delivery of doxorubicin by porous CaCO₃ and chitosan/alginate multilayers-coated CaCO₃ microparticles, *Colloid Surf. A* 353 (2010) 132–139.
- [36] D.V. Volodkin, N.I. Larionova, G.B. Sukhorukov, Protein encapsulation via porous CaCO₃ microparticles templating, *Biomacromolecules* 5 (2004) 1962–1972.
- [37] D.V. Volodkin, A.I. Petrov, M. Prev, G.B. Sukhorukov, Matrix polyelectrolyte microcapsules: new system for macromolecule encapsulation, *Langmuir* 20 (2004) 3398–3406.
- [38] L.N. Ramana, S. Sethuraman, U. Ranga, U.M. Krishnan, Development of a liposomal nanodelivery system for nevirapine, *J. Biomed. Sci.* 17 (2010) 1–9.
- [39] S. Latha, P. Selvamani, C. Senthilkumar, P. Sharavanan, G. Suganya, V.S. Beniwal, P. R. Rao, Formulation development and evaluation of metronidazole magnetic nanosuspension as a magnetic-targeted and polymeric-controlled drug delivery system, *J. Magn. Magn. Mater.* 321 (2009) 1580–1585.
- [40] J. Yang, S.B. Park, H.G. Yoon, Y.M. Huh, S. Haam, Preparation of poly-caprolactone nanoparticles containing magnetite for magnetic drug carrier, *Int. J. Pharm.* 324 (2006) 185–190.
- [41] L. Xie, X. Song, W. Tong, C. Gao, Preparation and structure evolution of bowknot-like calcium carbonate particles in the presence of poly(sodium 4-styrene sulfate), *J. Colloid Interf. Sci.* 385 (2012) 274–281.
- [42] Q. Sun, Z. Tong, C. Wang, B. Ren, X. Liu, F. Zeng, Charge density threshold for Lbl self-assembly and small molecule diffusion in polyelectrolyte multilayer films, *Polymer* 46 (2005) 4958–4966.
- [43] S. Raz, O. Testeniére, A. Hecker, S. Weiner, G. Luquet, Stable amorphous calcium carbonate is the main component of the calcium storage structures of the Crustacean *Orchestia cavimana*, *Biol. Bull.* 203 (2002) 269–274.
- [44] H.S. Nalwa, Encyclopedia for Nanoscience and Nanotechnology, American Scientific Publishers, USA, 2004, pp. 815–848.
- [45] Y. Wang, Y.X. Moo, C. Chen, P. Gunawan, R. Xu, Fast precipitation of uniform CaCO₃ nanospheres and their transformation to hollow hydroxyapatite nanospheres, *J. Colloid Interf. Sci.* 352 (2010) 393–400.
- [46] J.C. Yang, M.J. Jablonsky, J.W. Mays, NMR and FT-IR studies of sulfonated styrene-based homopolymers and copolymers, *Polymer* 43 (2002) 5125–5132.
- [47] P.E.G. Casillas, C.A.R. Gonzalez, C.A.M. Perez, Infrared Spectroscopy of Functionalized Magnetic Nanoparticles, Infrared Spectroscopy-Materials Science, Engineering and Technology Prof. Theophanides Theophile (Ed.) (2012) 405–420.
- [48] A.R. Chandak, P.R.P. Verma, Design and development of HPMC based polymeric films of methotrexate: Physicochemical and pharmacokinetic evaluations, *J. Pharm Soc. Japan* 128 (2008) 1057–1066.
- [49] P. Costa, J.M.S. Lobo, Modeling and comparison of dissolution profiles, *eur. J. Pharm. Sci.* 13 (2001) 123–133.
- [50] P.J. Flory, J. Rehner Jr., Statistical mechanics of cross-linked polymer networks II. Swelling, *J. Chem. Phys.* 11 (1943) 521–526.
- [51] T.H. Hai, L.H. Phuc, D.T.K. Dung, N.T.L. Huyen, B.D. Long, L.K. Vinh, N.T.T. Kieu, Contrast agents for magnetic resonance imaging based on ferrite nanoparticles synthesized by using a wet-chemical method, *J. Korean Phy. Society* 53 (2008) 772–775.
- [52] M.H.R. Farimani, N. Shahtahmassebi, M.R. Roknabadi, N. Ghows, Synthesis and study of structural and magnetic properties of super paramagnetic Fe₃O₄/SiO₂ core/shell nanocomposite for biomedical applications, *Nanomed. J.* 1 (2014) 71–78.